Volume 9 | Number 16 | 21 August 2022

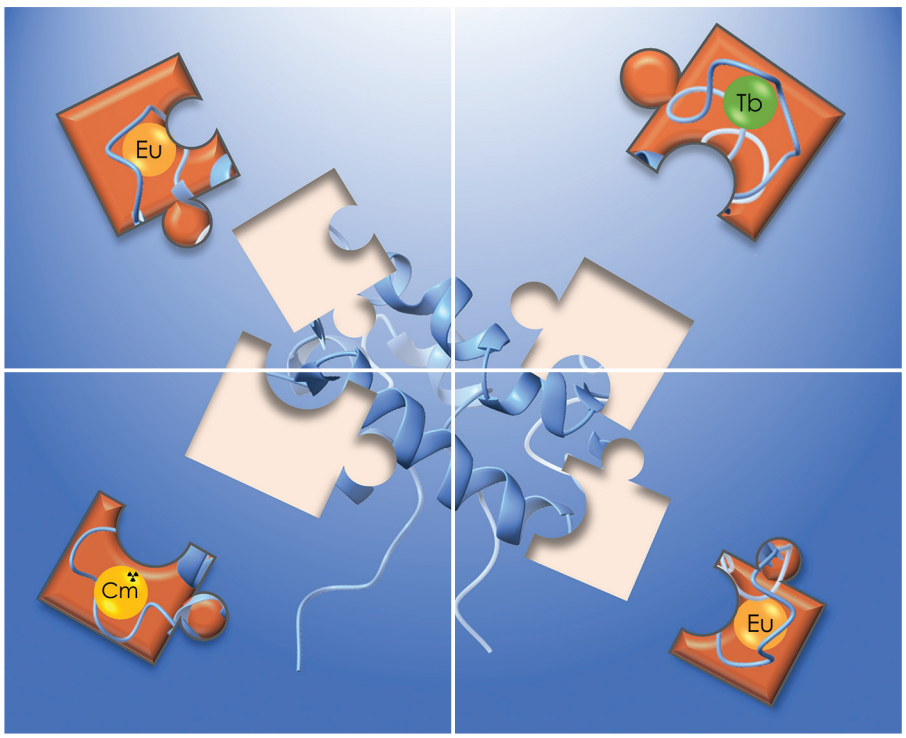

INORGANIC CHEMISTRY

FRONTIERS

CCS 中国化学会 CHINESE CHEMICAL SOCIETY
PEKING UNIVERSITY 1898
ROYAL SOCIETY OF CHEMISTRY
rsc.li/frontiers-inorganic

INORGANIC CHEMISTRY
FRONTIERS

RESEARCH ARTICLE

View Article Online
View Journal | View Issue

Cite this: *Inorg. Chem. Front.*, 2022, **9**, 4009

Lanmodulin peptides – unravelling the binding of the EF-Hand loop sequences stripped from the structural corset†

Sophie M. Gutenthaler, [a] Satoru Tsushima, [b,c] Robin Steudtner, [b] Manuel Gailer, [a] Anja Hoffmann-Röder, [a] Björn Drobot *[b] and Lena J. Daumann *[a]

Lanmodulin (LanM), a naturally lanthanide (Ln)-binding protein with a remarkable selectivity for Lns over Ca(II) and affinities in the picomolar range, is an attractive target to address challenges in Ln separation. Why LanM has such a high selectivity is currently not entirely understood; both specific amino acid sequences of the EF-Hand loops and cooperativity effects have been suggested. Here, we removed the effect of cooperativity and synthesised all four 12-amino acid EF-Hand loop peptides, and investigated their affinity for two Lns (Eu(III) and Tb(III)), the actinide Cm(III) and Ca(II). Using isothermal titration calorimetry and time-resolved laser fluorescence spectroscopy (TRLFS) combined with parallel factor analysis, we show that the four short peptides behave very similarly, having affinities in the micromolar range for Eu(III) and Tb(III). Ca(II) was shown not to bind to the peptides, which was verified with circular dichroism spectroscopy. This technique also revealed an increase in structural organisation upon Eu(III) addition, which was supported by molecular dynamics simulations. Lastly, we put Eu(III) and Cm(III) in direct competition using TRLFS. Remarkably, a slightly higher affinity for Cm(III) was found. Our results demonstrate that the picomolar affinities in LanM are largely an effect of pre-structuring and therefore a reduction of flexibility in combination with cooperative effects, and that all EF-Hand loops possess similar affinities when detached from the protein backbone, albeit still retaining the high selectivity for lanthanides and actinides over calcium.

Received 29th April 2022,
Accepted 23rd May 2022

DOI: 10.1039/d2qi00933a

rsc.li/frontiers-inorganic

Introduction

Lanthanides (Lns), the group of 15 elements at the centre of the periodic table, belong, together with Sc and Y, to the rare earth elements (REEs) and play a key role in our modern society.[1] These elements are essential in phosphors (*e.g.* LEDs, screens), strong permanent magnets (*e.g.* hard drives, phones, wind turbines) and rechargeable batteries, and are even found in medical applications (*e.g.* Gd(III) in MRI contrast agents).[2,3] Despite not being rare (apart from the radioactive promethium), as the misleading name REE indicates, Lns mostly co-appear in ores at low concentrations.[4] This and the chemical similarity within the series (prevalent oxidation state +III and similar ionic radii) make the mining, separation and purification of these elements extremely cumbersome.[1,4] Additionally, the procurement of Lns is also extremely harmful to the environment. The commonly used mining process involves harsh acidic or alkaline conditions leading to groundwater pollution by mobilising heavy metals from the ores as well as producing large amounts of radioactive waste (Lns often co-occur with actinides such as thorium and uranium).[2,3,5,6] This negative environmental impact is in strong conflict with the necessity of these elements for sustainable energy production. Therefore, greener solutions to satisfy the high demand for Lns are urgently needed. One suitable, more sustainable Ln-source, is believed to be found in End-of-Life (EoL) products.[7] However, similarly to the naturally occurring ores, Lns are used in combination with other elements and at low concentrations in those products. This highlights that for sustainable Ln acquisition, highly selective and effective methods are needed.

As nature has always been an inspirational source for scientists, it is convenient that Lns were found to be biologically essential less than 10 years ago with the finding of Op den Camp and co-workers, who first reported a Ln-dependent

[a]*Department of Chemistry Ludwig-Maximilians-University Munich Butenandtstraße 5-13, 81377 München, Germany. E-mail: lena.daumann@lmu.de*
[b]*Institute of Resource Ecology Helmholtz-Zentrum Dresden-Rossendorf e.V. Bautzner Landstraße 400, 01328 Dresden, Germany. E-mail: b.drobot@hzdr.de*
[c]*International Research Frontiers Initiative, Institute of Innovative Research, Tokyo Institute of Technology, Meguro 152-8550, Tokyo, Japan*
† Electronic supplementary information (ESI) available. See DOI: https://doi.org/10.1039/d2qi00933a

methanotrophic bacterium in 2014, opening up a completely new research field.[8] Nakagawa and co-workers had demonstrated earlier in 2012 that *M. extorquens* AM1 (abbreviated to AM1) can express a previously uncharacterised methanol dehydrogenase (MDH) upon addition of La(III) to the growth medium.[9] Along with SolV, this organism belongs to the ones best studied for their lanthanide metabolism.[10] In particular, *M. extorquens* AM1 is already strongly linked with bio-inspired REE-recycling strategies as it can, for example, directly leach Lns from magnet swarf.[11] Furthermore, AM1 has also been evolved to tackle the rising gadolinium levels in waterways, stemming from the widespread use of MRI contrast agents.[12]

In the past decade, it has been firmly established that Ln-using bacteria incorporate Lns in the active site of quinone-dependent MDH,[13,14] an enzyme class formerly only associated with calcium.[15–18] As calcium and Lns have similar ionic radii, chemists have used Lns as substitutes for calcium to investigate Ca(II)-binding proteins and enzymes by using the excellent spectroscopic properties of these metals long before it was discovered that Lns are biologically relevant.[19,20] Therefore, it is not surprising that the first discovered naturally occurring Ln(III)-binding protein, lanmodulin (LanM), isolated from *M. extorquens* AM1, belongs to the class of EF-Hand proteins, a protein class usually associated with binding strongly to calcium (see Fig. 1). The EF-Hand motif refers to a structural helix–loop–helix unit in which two alpha-helices are linked by a short 12-amino acid calcium(II)-binding loop.[21] LanM has four EF-Hands with metal-binding loops of which three have been reported to have a picomolar affinity for Lns and the fourth has lower, micromolar affinity.[22–24] The affinity for Lns has been demonstrated to be 100-million-fold higher for Lns than for calcium.[22] In addition, it was recently shown that LanM has a high affinity not only for Lns, but also for actinides (Ans).[25–27] Interestingly, all conducted studies observe a higher affinity of LanM for the Ans than for the Lns.[25–27]

Due to the aforementioned similarities between calcium and Lns, calcium-binding proteins such as calmodulin (CaM) have been used in the past as template for specific Ln-binding peptides.[28–31] Particularly noteworthy are lanthanide-binding tags (LBTs), which have been developed starting from EF-Hand binding loop sequences as a tool for analysing protein structures and protein–protein interactions by incorporating those short Ln-binding amino acid sequences (the LBTs) into the protein structure, which enables analysis *via* methods involving luminescence, NMR spectroscopy and others.[19,32–37] Additionally, uranyl-binding peptides, based on the EF-Hand sequences of CaM, are known.[38–40]

LanM, a protein, designed by nature to bind Lns with a high affinity for Ans, is an attractive target for the development of REE-recycling and Ans-separation methods.[24,26,27,41,42] With LanM as inspiration, *de novo* proteins,[43] peptides[44] and organic ligands can be envisioned. An example of such a bio-inspired approach is the use of pyrroloquinoline quinone (PQQ; the cofactor of the aforementioned Ln-MDHs) in the separation of Lns by precipitation in aqueous solution.[45] A key step in using natural ligand design as a foundation to develop potent Ln-binding ligands is understanding why, for example, certain amino acid sequences or structural motifs are beneficial. For CaM numerous extensive studies and systematic analyses of which amino acid combinations in which positions are most common in CaM and related proteins were conducted.[21,46] Features that decrease Ca(II) affinity while increasing the affinity towards Lns or other trivalent ions have already been reported in the literature.[47–49] Remarkably, some

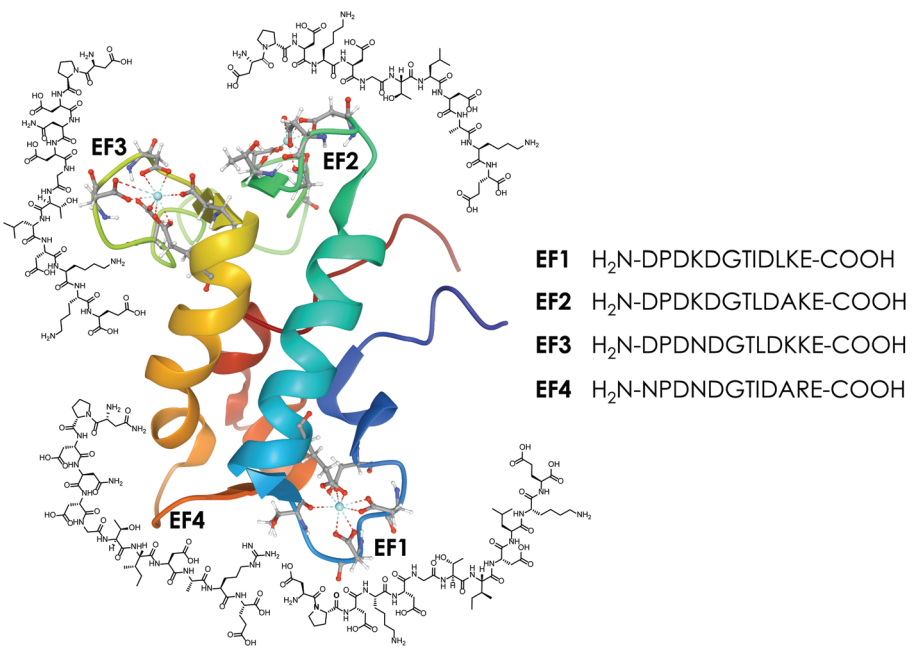

Fig. 1 The protein LanM (PDB 6mi5) and the four synthesised EF-Hand loop peptides (named after the four EF-Hands of the full protein LanM) investigated in this study.

of these features can be found in lanmodulin. For example, aspartic acid can be found in the ninth position in all four EF-Hands of lanmodulin[22] and the presence of an acidic amino acid in this specific position has already been shown to be beneficial in order to decrease the Ca(II) selectivity and increase the affinity for trivalent ions.[47–49] However, aspartic acid in position nine is not highly uncommon in canonical EF-loops as this position is occupied by Asp in almost a third of CaMs and CaM-like proteins.[21] More unusual is the presence of proline in position two (again in all four LanM EF-Hands), which is why it was suggested by Cotruvo and co-workers[22] that this might be one reason for lanmodulin's unique features. This has already been investigated on the protein level *via* molecular dynamics simulations and 2D IR.[50] The authors found when exchanging the proline in position two against an alanine that the selectivity for the early lanthanides decreases. This was attributed to the resulting higher flexibility of the binding site, which can bind to a broader range of ions, highlighting the proposed role of proline. Interestingly, this is also supported by a study published in 2004 [51] in which 36 amino acid-long helix–loop–helix peptides derived from a Ca(II)-binding EF-Hand protein were investigated, revealing that by replacing a proline residue with glycine, the affinity for Ca(II) can be further increased, demonstrating that the presence of proline decreases the selectivity for Ca(II) and increases the selectivity for trivalent ions. The lower affinity of EF-Hand 4 in LanM is suggested to be mainly due to the presence of an asparagine residue in position one (EF1–EF3, D at position 1), which is normally occupied by an aspartic acid residue in EF-Hand proteins.[21]

One possibility to take a closer look at the differences between LanM's four binding loops fully detached from cooperativity and other effects generally observed in proteins, such as pre-structuring *etc.*, is to take the protein apart and look at it on the peptide level.

Therefore, this study brings us one step closer to understanding LanM high affinity for Lns by comparing the EF-Hand-binding loops as four isolated 12-amino acid peptides (see Fig. 1). We use time-resolved laser-induced fluorescence spectroscopy (TRLFS), circular dichroism (CD) spectroscopy, isothermal titration calorimetry (ITC) and molecular dynamic (MD) simulations to investigate the metal-binding properties of the four LanM-based peptides with Eu(III), Tb(III), Cm(III) (selected as representatives of Lns and Ans based on their excellent fluorescence properties) and Ca(II) and thereby contribute to understanding of the differences between the four metal-binding sites in the full protein.

Experimental

Detailed documentation of all experimental procedures and experiments performed can be found in the ESI.† The ESI† is divided into different sections covering the reagents used, peptide synthesis and purification, peptide purity and concentration determination, experimental protocols for the performed binding studies *via* CD, ITC and TRLFS, including the performed data analysis steps, and a description of the performed MD simulations.

Results and discussion

Synthesis, purification and determination of the target peptide concentration

In this study a total of four 12-amino-acid peptides based on the four metal-binding EF-Hand loops (numbered 1–4, see Fig. 1) of the naturally occurring Ln-binding protein LanM were synthesised *via* automated microwave-assisted solid-phase peptide synthesis (SPPS) using *Fmoc* conditions. For all peptides a preloaded Wang resin that gives a C-terminal carboxylic acid was used. The C-terminal carboxylic acid was preferred over a terminal amide function, as an additional carboxylic group was expected to be beneficial for binding lanthanides. As all four sequences contain at least one amino acid combination (*e.g.* Gly–Asp) that is prone to aspartimide formation,[52–55] 5% formic acid was added during the *Fmoc* deprotection step to minimise the formation of unwanted side products as recommended in the literature.[56] With these conditions, all four sequences were successfully synthesised as determined by mass spectrometry and purified using preparative RP-HPLC (Chapter 2, ESI†). As no sequence contained a tryptophan side chain or an aromatic residue in general, the absorption at 280 nm could not be used to determine the net peptide concentration. Therefore, the target peptide concentration was obtained using the Pierce™ quantitative fluorometric peptide assay, taking the purity determined using analytical HPLC into account. The determined concentration was later corrected with a correction factor *N* determined by ITC (Section 4.3, ESI†), as the analysis suggested a slight underestimation of the real peptide concentration using the method described above.

Eu(III)- and Ca(II)-binding to the EF-Hand loop peptides

First, the binding properties of the four peptides to Eu(III) and Ca(II) were examined, as one interesting feature of LanM mentioned in the literature[22] is the significantly higher affinity for lanthanides over Ca(II). The investigations were started with ITC experiments in which Eu(III) was added in increasing amounts to the respective peptide. The obtained thermogram and integrated heat plot of the Eu(III)/EF1 titration experiment are shown as an example in Fig. 2.

The data can be fully explained by the formation of three species: a 2 : 1, a 1 : 1 and a 1 : 2 peptide to Eu(III) complex. The formation of the 2 : 1 peptide to Eu(III) complex is suggested by the slight increase in enthalpy at the beginning of the titration. With increasing Eu(III) concentration the first dominant species is the 1 : 1 peptide to Eu(III) complex, whereas at high Eu(III) concentration a 1 : 2 peptide to Eu(III) complex seems to be formed, which is responsible for the slight offset between the initial fit and the raw data when only considering a 1 : 1 complex. However, the 2 : 1 peptide to Eu(III) complex is not dominant and not present in significant amounts, which is

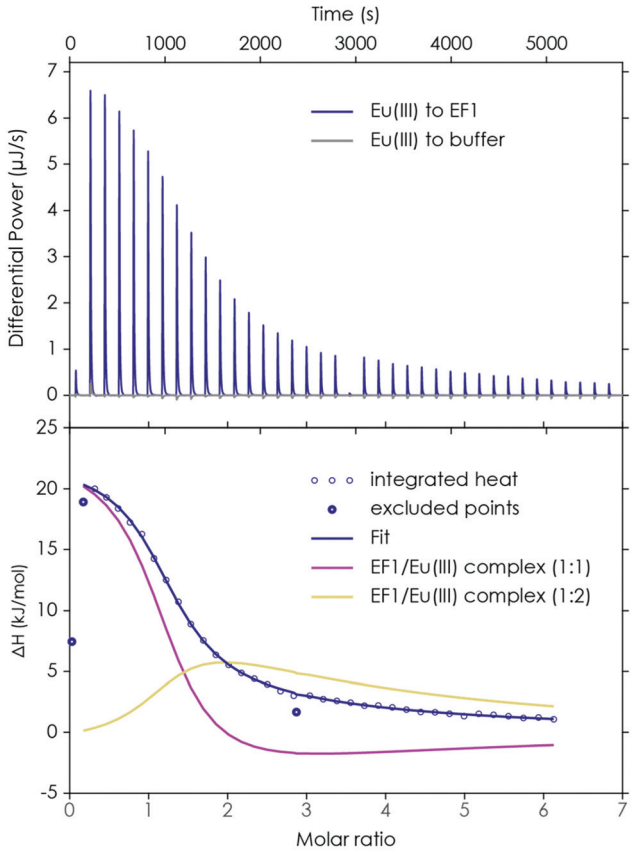

Fig. 2 ITC of EF1 binding to Eu(III). Upper panel: thermogram obtained by performing a titration of 1.5 mM Eu(III) to 100 µM EF1 at pH 6.6 (10 mM MOPSO, 100 mM KCl) and the corresponding background measurement (Eu(III) to buffer). Lower panel: integrated heat and best fit with a 2-component model. Data points which are displayed as circles were excluded from the analysis.

why it was not possible to fully thermodynamically characterise it (compare with Section 4.3 of the ESI and Fig. S4† for more details). Therefore, this species was neglected during the final analysis by excluding the second titration step and only fitting the 1 : 1 and 1 : 2 peptide to Eu(III) complexes (see Fig. 2 and Fig. S6–S9† for the 2-component analysis). For the 1 : 1 peptide to Eu(III) complexes the reaction enthalpy (ΔH) is slightly higher than for the 1 : 2 complexes. In general, for all four peptides very similar values ($\Delta H_{1:1}$ = 20–24 kJ mol^{-1} for EF1–EF4; $\Delta H_{1:2}$ = 21–19 kJ mol^{-1} for EF1–EF3) were obtained. Solely for the 1 : 2 complex of EF4, a lower reaction enthalpy can be observed (13 kJ mol^{-1}). For the 1 : 1 complexes the Gibbs energy (ΔG) is around −29 kJ mol^{-1} and for the 1 : 2 complexes it is around −20 kJ mol^{-1}, showing that for both the complex formation is thermodynamically favourable, which suggests, together with the observed endothermic behaviour, an entropy-driven binding event. Not only the metal-binding process, but also the stripping of the first and second hydration shells of the Eu(III) aquo ion (increase in entropy),[49] as well as the presumed dehydration of the peptide (increase in entropy) in addition to structural changes upon metal binding, contribute to the final thermogram. As the complex formation is similarly exergonic for all peptides, the lower enthalpy of the 1 : 2 EF4 to Eu(III) complex goes hand in hand with a lower entropic component (ΔH, ΔG, and $-T\Delta S$ for both species are shown in Table S4†). In addition to the thermodynamic variables, the determined complex binding affinities (K_D) show very similar values for all four peptides. For the formation of a 1 : 1 complex the Eu(III) affinity is in the lower micromolar range (around 8.5 µM), while the affinity for the formation of a 1 : 2 complex is significantly lower (see Table 1). This is interesting as at least for EF4 – the proposed low-affinity site in LanM[22] – a lower affinity was expected. However, on the amino acid level no significant differences between the four EF-Hands could be determined. This suggests that the different binding affinities for the four binding loops in LanM are not primarily caused by differences in the amino acid sequences, but dominated by cooperative effects.

The observations made by ITC were confirmed and investigated in depth by TRLFS titration experiments. One advantage of this method is that very low concentrations can be used, perfectly suited to investigating affinities in the micromolar or even nanomolar range while using only small sample amounts. Furthermore, the number of bound water molecules can be estimated, giving first hints towards how many amino acid residues are involved in the metal binding as well as structural insights. This method has already been applied successfully for the investigation of CaM and LanM in the literature.[25,57] In general, the metal-binding information is obtained due to spectral deconvolution by parallel factor analysis (PARAFAC), which is a robust analytical tool for determining unique explanatory factors directly.

For comparison the first set of experiments was performed by adding an Eu(III) solution to the respective peptide in solution (the analysed data for the Eu(III)/EF1 experiment are shown in Fig. 3A and B). The analysis of these experiments strongly supports the formation of two different peptide to Eu(III) complexes, as suggested by ITC. A comparison of the chemical species distribution obtained by those two methods is shown in Fig. 4. The species distributions are, especially for the 1 : 1 complex, in good agreement and show in general a

Table 1 K_D values obtained by Eu(III) to EF titration experiments *via* ITC and TRLFS. The ITC values are averaged from two independent experiments using different concentrations; the deviation between both experiments is given as the error. The given error for the TRLFS data is the standard deviation. Conditions for ITC and TRLFS: 25 °C, pH 6.6 in 10 mM MOPSO buffer with an ionic strength of 100 mM KCl

	K_D (µM) measured by ITC		K_D (µM) measured by TRLFS	
EF–Eu(III) complex	1 : 1	1 : 2	1 : 1	1 : 2
EF1	8.55 ± 0.17	325 ± 93.0	4.39 ± 2.21	30.5 ± 12.7
EF2	8.61 ± 0.04	309 ± 49.5	4.44 ± 0.82	36.9 ± 3.17
EF3	8.02 ± 1.23	511 ± 169	3.05 ± 2.83	20.5 ± 10.7
EF4	8.85 ± 0.16	456 ± 229	2.42 ± 1.94	50.5 ± 19.3

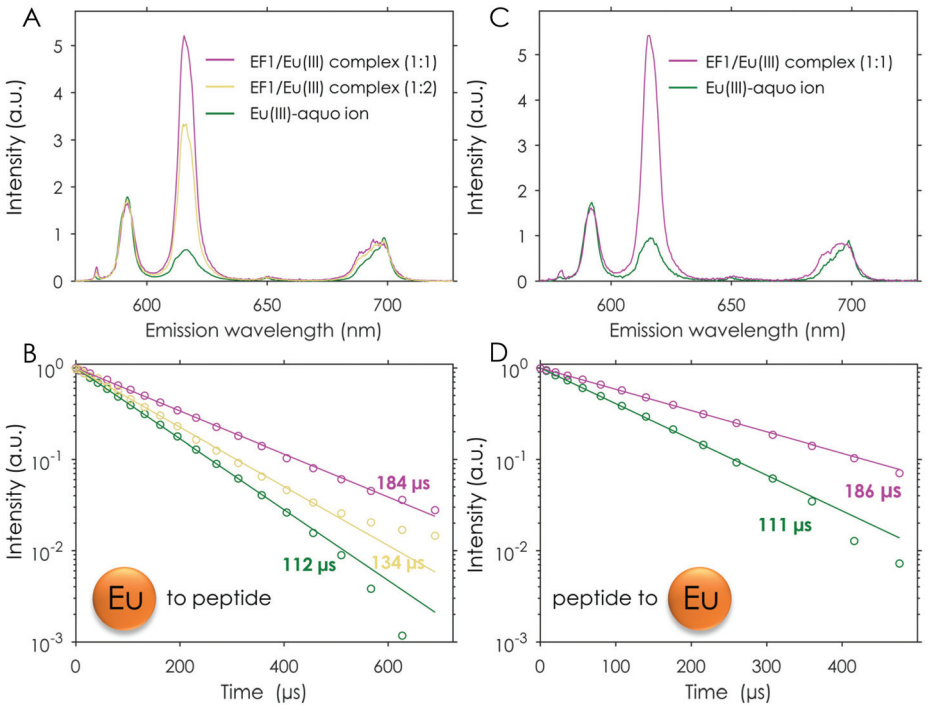

Fig. 3 TRLFS titration experiment of Eu (0–122.5 µM) to EF1 (12 µM) at pH 6.6 (10 mM MOPSO, 100 mM KCl), λ_{ex} (Eu) = 394 nm. (A) Deconvoluted spectra and (B) lifetimes of the three observed species. TRLFS titration experiment of EF1 (0–27.4 µM) to Eu (0.5 µM) at pH 6.6 (10 mM MOPSO, 100 mM KCl), λ_{ex} (Eu) = 394 nm. (C) Deconvoluted spectra and (D) lifetimes of the two observed species.

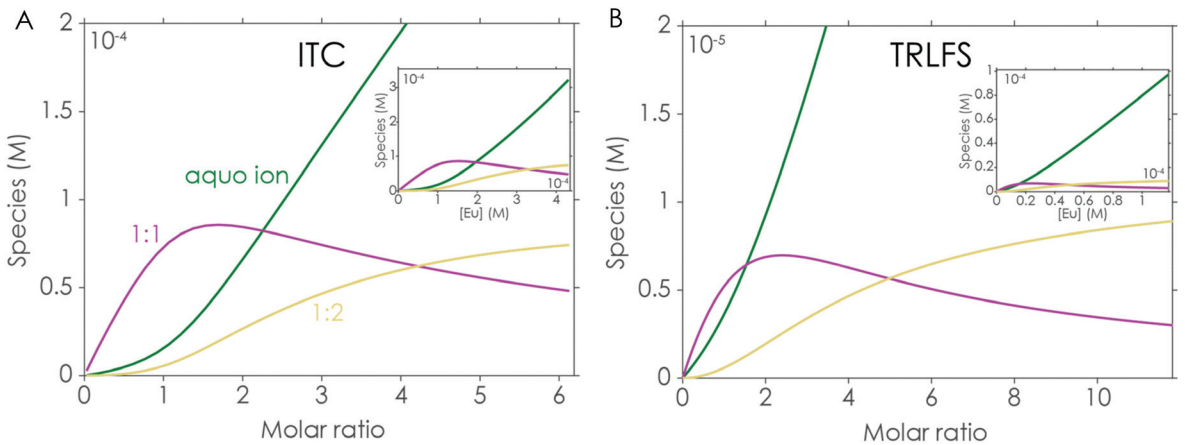

Fig. 4 Chemical species distribution observed in Eu(III) to EF1 titration experiments *via* ITC (A) and TRLFS (B), the corresponding ITC and TRLFS data are shown in Fig. 2 and 3A/B.

similar trend for both methods. The K_D values determined by TRLFS (see Table 1) for the 1 : 1 complex are of the same order of magnitude as the values obtained for the ITC experiment while a larger offset for the 1 : 2 complex can be observed. In general, the accuracy of stability constants for stepwise complexation decreases with increasing stoichiometry, since the value for the complex with higher stoichiometry depends on the value of the precursor complex. Furthermore, differences in the K_D values (and thus speciation) between the two methods are likely due to the different set-ups. Since there are no precise pK_a values for the coordinating functional groups, we are providing K_D values instead of log(β) values – such affinities depend on system compositions, *e.g.* concentration regimes.

The formation of a 2 : 1 peptide to Eu(III) complex as indicated by ITC could not be confirmed by TRLFS. This is not unexpected as this complex would be expected to only form at very low Eu(III) concentrations in comparison with the respective peptide, thus this species remains elusive with this method.

Table 2 K_D values and lifetimes (τ) obtained by EF to metal TRLFS titration experiments. The number of coordinated water molecules (q) was calculated for Eu(III) and Cm(III) using the equations established by Kimura,[66] based on work of Horrocks[67]

	EF–Eu(III) 1 : 1 complex		EF–Tb(III) 1 : 1 complex		EF–Cm(III) 1 : 1 complex	
	K_D (μM)	τ (μs)/q_{water}	K_D (μM)	τ (μs)	K_D (μM)	τ (μs)/q_{water}
EF1	5.50 ± 0.57	186.2 ± 3.7/5.1	8.47 ± 0.325	450 ± 18.0	2.28 ± 0.104	143.1 ± 19/3.7
EF2	6.52 ± 0.48	181.8 ± 8.6/5.3	8.24 ± 1.31	469 ± 5.30	2.86 ± 0.084	147.7 ± 18/3.5
EF3	7.42 ± 1.04	182.1 ± 2.2/5.3	8.46 ± 0.864	502 ± 11.0	2.77 ± 0.229	137.4 ± 15/3.9
EF4	7.56 ± 1.49	186.3 ± 4.3/5.1	7.85 ± 1.23	502 ± 4.00	2.34 ± 0.088	142.7 ± 3.0/3.7

Generally, it is more beneficial for TRLFS experiments to titrate the peptide to the metal solution. Using this set-up solely the 1 : 1 complex could be observed (see Fig. 3C and D). The obtained lifetimes match those found in the reverse titration experiment for the 1 : 1 complexes described earlier (compare Fig. 3B and D and Table S5† and Table 2).

Next, the Ca(II)-binding affinity of the four peptides was examined using ITC, TRLFS and CD titration experiments. In contrast to the ITC experiments with Eu(III), the addition of Ca(II) to the peptide solutions showed no complex formation, even though the added Ca(II) concentration was five times the amount used in the Eu(III) set-up. The obtained thermograms hardly deviated from the background titrations (Fig. S10 and S11†). This clearly shows that *via* ITC no Ca(II) binding to the peptides could be observed. However, an affinity in the molar range cannot be fully ruled out with this technique, as ITC is better suited to systems with an affinity in the millimolar to nanomolar range. One could conclude, based on this first comparison between Ca(II) and Eu(III), that the high selectivity for Lns over Ca(II) for which LanM is known[22] is preserved in the short amino acid sequences of the binding loops. However, a significantly lower Ca(II) affinity of short EF-Hand-based peptides is to be expected, based on the available literature on Ca(II)-binding protein-inspired small peptides. It has been shown multiple times that the Ca(II) affinity is significantly reduced in such peptides and strongly depends on the length of the amino acid chain. For most of the reported 12 AA peptides no Ca(II) affinity or solely a low affinity in the millimolar range is reported while longer peptides (starting at around 20 AA) have affinities in the higher micromolar range.[58–61] One reason for the absence of even a millimolar affinity between Ca(II) and the LanM peptides could be the proline residue at position two. It was shown as early as 2004 that the presence of a proline residue significantly reduces the affinity for Ca(II) in protein-inspired peptides.[51]

The observations made using ITC for the Ca(II) binding affinity were further confirmed by TRLFS experiments. For this, Eu(III) was added to a sample containing EF1 and a high excess of Ca(II). The analysis showed no significant differences for the Eu(III) to EF1 dataset (compare Fig. 3A/B and Fig. S13†) despite the high concentration of Ca(II) present. The spectral deconvolution yielded again the presence of three species, the free Eu(III) aquo ion, a 1 : 1 and a 1 : 2 peptide/Eu(III) complex, each with lifetimes matching the values obtained earlier within the experimental error (compare Table S5, Table S6† and Table 2).

In addition, the influence of Eu(III) and Ca(II) on the structure of the four peptides was investigated *via* CD spectroscopy. For this, titration experiments in which the peptide concentration was kept constant while the metal concentration was increased were performed. The obtained spectra are shown in Fig. 5. In the absence of Ca(II)/Eu(III) the CD spectrum shows for all peptides a distinct minimum around 200 nm and a slight shoulder at 222 nm, suggesting a random-coil conformation with very few secondary structure elements.[62] The addition of Eu(III) in increasing amounts leads to a slight decrease in (molar) ellipticity at 222 nm and a slight increase in (molar) ellipticity at around 200 nm. Isodichroic points are visible around 210 nm. The decrease in (molar) ellipticity at 222 nm is associated with an increase in α-helicity caused by metal binding, as reported in the literature.[28,29,31,63,64] The observed changes appear to increase within the peptide series from EF1 to EF4. The first two EF-Hand peptides as well as EF3 and EF4 show very similar changes in the CD upon Eu(III) addition. EF4 shows slightly more secondary structure content at an excess of Eu(III) in comparison with *e.g.* EF1 when looking at the (molar) ellipticity at around 220 nm and 222 nm. However, no shift in the minimum at 220 nm towards 210 nm, which would be typical for larger peptides/proteins with a high α-helical content, can be observed.[62] When normalising the change in ellipticity at 222 nm with respect to the Eu(III) amount, a very similar progression for all four peptides can be observed (Fig. S5C†), suggesting that the peptides undergo structural changes to a similar degree at the same Eu(III) equivalents, supporting the observed similar binding affinities. In contrast to Eu(III), the addition of Ca(II) does not trigger any conformational change for any of the peptides. This again strongly supports the conclusions drawn from the ITC and TRLFS experiments: at the tested conditions the LanM peptides do not bind Ca(II) to a significant degree.

As the CD experiment clearly showed a structural change upon Eu(III) addition, the experimental observations were further investigated by molecular dynamics simulations. Calculations of the four EF-Hand loop peptides were performed using two different sets of initial structures. A first set of MD simulations was performed by taking the local structures of the EF-Hand loop from the NMR structure of LanM[23] (PDB 6mi5) and removing the residual protein. As the metal-binding loop of EF-Hand 4 is not occupied with a metal in the structure for the peptide EF4, the NMR structure of EF-Hand loop 1 was taken and the sequence "mutated". These calcu-

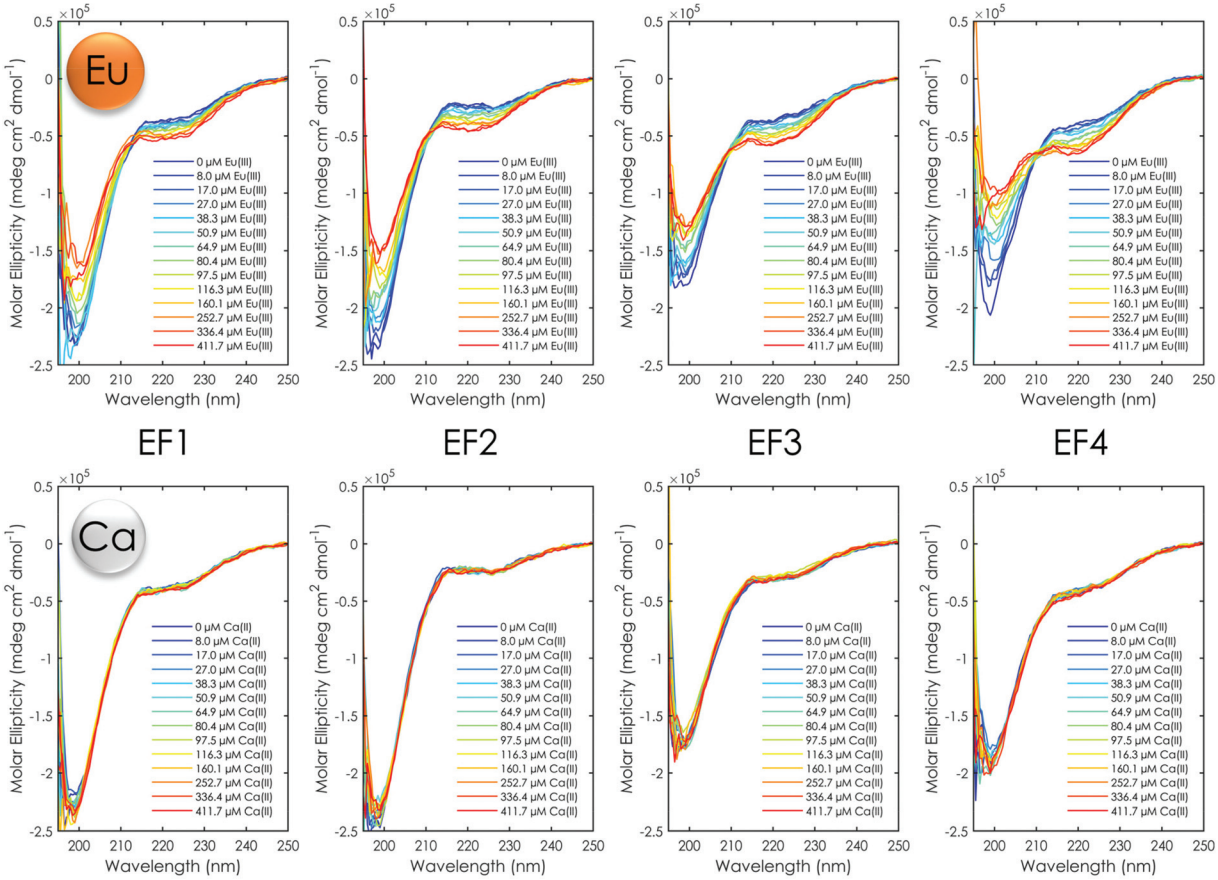

Fig. 5 CD spectra of Eu(III) (top) and Ca(II) (bottom) titration experiments with all four EF-Hand peptides at pH 6.6 (10 mM MOPSO, 100 mM KCl).

lations converged to structures (Table S9†) in which Eu(III) is fully coordinated by amino acid residues and there is virtually no water except for EF4 in which two water molecules are coordinated to Eu(III). These calculations show the high potential of the amino acid sequence for Ln(III) coordination, but from our experimental observations it became clear that these calculations do not match the experimental evidence. From the experiments we observed micromolar binding affinity for Eu(III) with about 5 water molecules completing the Eu(III) coordination sites when in a 1 : 1 complex (calculated from the luminescence lifetimes, see Table 2 and Table S5†) as well as very few secondary structural elements in the absence of metal, which increases upon Eu(III) binding (Fig. 5). Therefore, a more realistic set of simulations was performed in the presence and absence of Eu(III) without any initial restraints. Each peptide was initially prepared as a "string" having the sequences of the corresponding EF-Hand loop and was allowed to freely wrap around Eu(III). This second set of simulations converged to a totally different set of structures than the first simulation experiment, thereby better matching the experimental data. Eu(III) is coordinated over fewer amino acid residues and on average by about four to five water molecules (Table S10†). RMSD (root-mean-square deviation) plots of the simulations for EF1 with and without Eu(III) show that that the

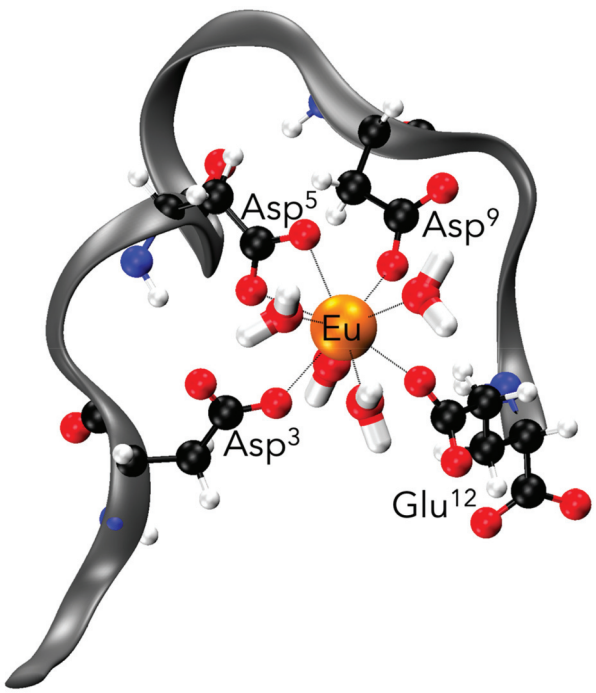

Fig. 6 Representative ball-and-stick drawing of Eu(III)-bound EF-Hand 1 from the MD trajectory. Grey ribbon depicts the peptide backbone (orange, Eu; blue, N; black, C; red, O; white, H).

structure with Eu(III) has converged well (Fig. S19†). The coordination of EF1 to Eu(III) based on the simulations is shown in Fig. 6.

Even though the association of the peptides with the metal is only through 2 to 4 residues (in contrast to 5 to 6 residues in structures obtained when starting from the NMR solution structure), the peptide structure is well preserved during the simulation in comparison with those without metals (Fig. 7). In the absence of Eu(III) the peptide flexibility is very high and retains ill-defined secondary structures, and only after the addition of Eu(III) upon metal binding is a more organised structure obtained, which is in good agreement with the observations made using CD spectroscopy (compare Fig. 5 and 7). This observation is also further confirmed through DSSP analysis (Define Secondary Structure of Proteins, a hydrogen bond estimation algorithm) of the MD trajectories (Fig. S18†). At this point a recently published new set of 12-6-4 Lennard–Jones-type parameters should be mentioned, which has been developed to reproduce binding energies for La(III), Y(III), Ca(II) and Mg(II) and tested on the EF-Hand loop EF1 of LanM and CaM.[65] However, as these simulations were not performed for Eu(III) and starting from the NMR solution structure geometry, no comparison can be drawn here.

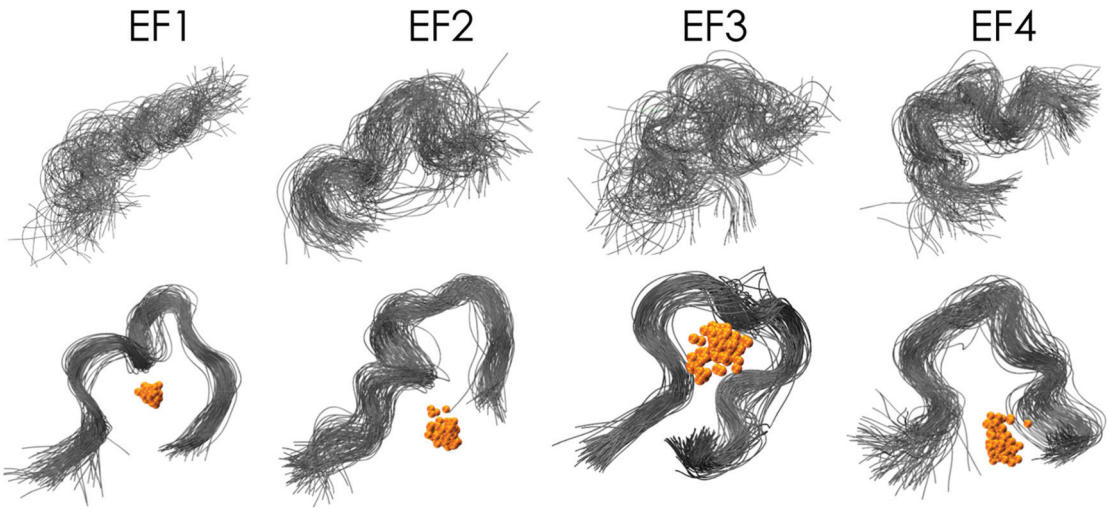

Fig. 7 Superimposed MD snapshots of metal-free (top panel) and Eu(III)-bound (lower panel, Eu in orange) bound to EF-Hand loop peptides (grey ribbon) for every 1 ns of the 100 ns MD trajectory (waters excluded from display).

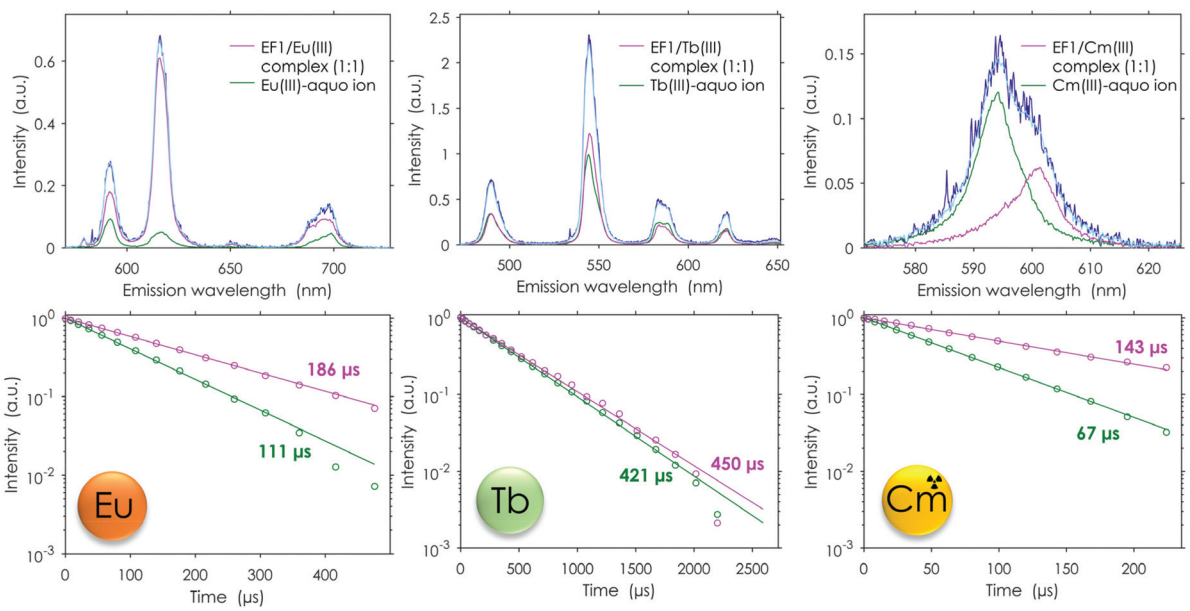

Fig. 8 TRLFS data: spectral deconvolution (top) and lifetimes (bottom) for the peptide to metal titration experiments (Eu/Tb pH 6.6; Cm 6.0,[a] 10 mM MOPSO, 100 mM KCl); light blue = full spectrum obtained by the used model, dark blue = raw spectrum; λ_{ex} (Eu) = 394 nm, λ_{ex} (Tb) = 220 nm, λ_{ex} (Cm) = 396 nm. [a] pH needed to be adjusted as at a pH of 6.6 not solely the free Cm(III) aquo ion was observed.

Eu(III) binding compared with Tb(III) and Cm(III) binding

In addition to the extensive metal-binding studies using Eu(III), this study was further complemented by including another Ln, terbium. Furthermore, the binding properties of the EF-Hand loop peptides were tested with the actinide curium to see whether the even higher affinity of Ans over Lns which was observed for lanmodulin[25–27] is also preserved in the short peptides. The comparison between the different metals with EF1 as an example can be seen in Fig. 8. In contrast to Eu(III), Tb(III) does not show hypersensitivity like the $^5D_0 \rightarrow {}^7F_0$ transition of Eu(III). A change in the coordination sphere causes only minor changes in the shape of the emission spectrum. Therefore, a direct readout of the Tb(III) interaction is complicated, and usually its complexation is only traced by changes in its lifetime. Here we can show that minor changes in the emission spectra combined with the changes in the luminescence lifetimes can be used to decompose TRLFS Tb(III) titration experiments using PARAFAC, thereby demonstrating its suitability for the methods described here. The experiment with Tb(III) further confirmed the Eu(III) experiments by showing the formation of one 1 : 1 complex. The obtained K_D values are also in the lower micromolar range, suggesting a very similar binding affinity for Tb(III) as well as Eu(III) (see Table 2). Overall, the Tb(III) titrations strongly support the observations already made with Eu(III).

The analogously conducted experiment with Cm(III) again pointed out the similarity of the four different peptides: the binding affinities for Cm(III) are in the same range (Table 2). A comparison of Cm(III) and Eu(III) luminescence lifetimes after interaction with the full protein[25] and isolated EF-Hand loop peptides further supports the current conclusions from experiment and simulation. The luminescence lifetimes were significantly shorter for the EF-Hand loop peptides compared with the full protein (180 μs *vs.* 370 μs [25] for Eu(III) and 140 μs *vs.* 200 μs [25] for Cm(III)). This indicates more water and less peptide functionalities in the first coordination sphere of the metal centre. The analysis suggested that the affinity for Cm(III) is slightly higher than for both investigated lanthanides (2–3 μM). In addition to the fitted affinity the calculated water molecules based on the luminescence lifetime also show on average one water molecule less, which is coordinated to Cm(III) when compared with Eu(III), again indicating a tighter binding. This nicely fits into the observations made in the literature for LanM, which all showed that the naturally Ln-binding protein favourably binds actinides.[25–27] Our data show that this preference is preserved even in these short peptides.

Binding competition: lanthanide *versus* actinide

To confirm the higher affinity for Cm(III) over Tb(III) and Eu(III) found in TRLFS experiments, a "fair"‡ competition experiment was envisioned in which the peptides were added in increasing amounts to a solution containing the same concentrations of Cm(III) and Eu(III). To the best of our knowledge, this is the first time that such an experiment in which both metals are simultaneously probed has been performed. One difficulty in such a set-up is the higher sensitivity of Cm(III) (higher quantum yield) in comparison with Eu(III). To optimise the weighting of the detected signal towards Eu(III), the excitation wavelength of Eu(III) was chosen for both metals. This was important, as both the Cm(III) and the Eu(III) emissions superimpose, which makes the data deconvolution challenging. Nevertheless, we were able to analyse the measured data using PARAFAC and obtained single component emission spectra, the corresponding lifetimes and the speciation. The analysis showed the expected formation of the 1 : 1 peptide/Eu(III) and peptide/Cm(III) complexes as well as the presence of the respective free aquo ions (see Fig. 9). In this direct setting, we were able to confirm the slightly higher affinity for Cm(III) over Eu(III) discussed above.

In the future, modifications of the natural EF-Hand loop peptides towards higher selectivity for Ans over Lns can be envisioned. It has already been shown in the literature[68] for

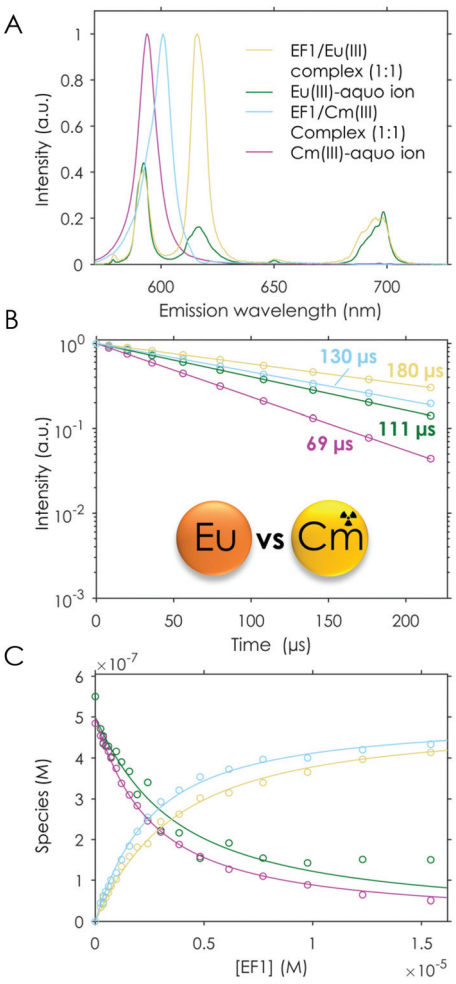

Fig. 9 TRLFS data of the titration experiment of EF1 to Cm(III)/Eu(III), λ_{ex} (Eu/Cm) = 393.9 nm. (A) Spectral deconvolution of the different species, (B) lifetimes and (C) speciation; the legend given in (A) applies to (B) and (C).

‡Fair is set in quotes to highlight that such an experiment also has limitations due to the different sensitivities of Eu(III) and Cm(III).

LBTs that by substituting the aspartic acid in position 5 with a cysteine or a 2-methylenepyridine group, the selectivity for Ans over Lns can be increased by a factor of 10.

Although the affinity of the peptides compared in this study is significantly reduced when compared with the full protein LanM, remarkable affinities for such short peptides were reached. For the full protein calmodulin, a natural Ca(II)-binding protein which also has a higher affinity for Lns/Ans than Ca(II), similar average K_D values are reported in the literature[57] (6.6 μM for Eu(III)) as for the isolated EF-Hand loop peptides of LanM. This indicates the great potential of these sequences in f-element accumulation processes as required by *e.g.* efficient recycling strategies.

Conclusions

In this study an extremely consistent picture of the Ln- (Eu(III) and Tb(III)) and An-binding (Cm(III)) capabilities of the LanM-based 12-amino acid peptides (EF-Hand loops) could be drawn. We were able to show that the Ln affinity, the preference for actinides and the low affinity for Ca(II) are preserved even in these short peptide sequences. Although the high affinity of LanM, which has been reported[22] to be in the picomolar range, is not observed for its EF-Hand loop peptides, their affinity is remarkably high, especially considering that they are not modified or optimised. These short peptides even reach affinities in the micromolar range, similar to the average affinity of the four calmodulin binding sites, which are known to also have a higher affinity for Eu(III) and Cm(III) over Ca(II).[57] Furthermore, the investigation without cooperative and pre-structuring effects of the full protein enabled us to study the impact of the amino acid sequence on the Ln affinity. We show that all four peptides behave very similarly, strongly supporting the assumption that the major differences in Ln affinity observed in the literature[22,24] for the different EF-Hands are mainly due to cooperativity, hydrogen bonding, pre-structuring and the decreased flexibility of the full protein. In summary, this work presents a good starting point for the development of selective and highly affine peptides. These could, once optimised, find application in medicine, recycling and An/Ln separation.

Data availability

The authors declare that the data supporting the findings of this study are available within the paper and its ESI.† In addition, full raw and processed TRLFS and ITC datasets as well as the used MATLAB code are available at **https://cloud.hzdr.de/s/6dkiJBeDenzy5f6** (password: EF-Hand_Sophie_1).

Author contributions

LJD and SMG conceptualised the idea and wrote the initial draft of the manuscript. LJD acquired funding for the project; all authors were involved in reviewing and editing this manuscript. SMG and MG synthesised the peptides. SMG purified and analysed the peptides and determined the purity and concentration. SMG acquired and analysed CD spectroscopy data. SMG and BD acquired the ITC data. SMG, BD, RS acquired the TRLFS data and conducted lanthanide and actinide titrations. BD fitted the ITC and TRLFS data. ST performed the molecular dynamic simulations and provided the interpretation. LJD, RS and AHR provided the necessary resources and infrastructure for this work.

Conflicts of interest

There are no conflicts to declare.

Acknowledgements

SMG thanks the Studienstiftung des Deutschen Volkes e.V. for funding through a PhD scholarship, the Münchner Universitätsgesellschaft e.V. for funding, Manuel Gebauer for his support with the peptide purifications and Falk Lehmann for conducting spontaneous MS measurements at the HZDR. LJD acknowledges the ERC Starting Grant Lanthanophor (945846) and the Klaus Tschira Boost Fund. Furthermore, the authors wish to thank the TU Dresden for computation time as all MD calculations were performed at the Centre for Information Services and High-Performance Computing (ZIH) at the Technische Universität Dresden. Additionally, the authors wish to thank Professor Peter Klüfers for access to the CD Instrument.

References

1 T. Cheisson and E. J. Schelter, Rare earth elements: Mendeleev's bane, modern marvels, *Science*, 2019, **363**, 489–493.
2 V. Balaram, Rare earth elements: A review of applications, occurrence, exploration, analysis, recycling, and environmental impact, *Geosci. Front.*, 2019, **10**, 1285–1303.
3 Z. Weng, S. M. Jowitt, G. M. Mudd and N. Haque, A detailed assessment of global rare earth element resources: Opportunities and challenges, *Econ. Geol.*, 2015, **110**, 1925–1952.
4 J. H. L. Voncken, *The Rare Earth Elements: An Introduction*, Springer International, 2015.
5 N. Haque, A. Hughes, S. Lim and C. Vernon, Rare earth elements: Overview of mining, mineralogy, uses, sustainability and environmental impact, *Resources*, 2014, **3**, 614–635.
6 S. H. Ali, Social and environmental impact of the rare earth industries, *Resources*, 2014, **3**, 123–134.
7 S. M. Jowitt, T. T. Werner, Z. Weng and G. M. Mudd, Recycling of the rare earth elements, *Curr. Opin. Green Sustainable Chem.*, 2018, **13**, 1–7.

8 A. Pol, T. R. M. Barends, A. Dietl, A. F. Khadem, J. Eygensteyn, M. S. M. Jetten and H. J. M. Op den Camp, Rare earth metals are essential for methanotrophic life in volcanic mudpots, *Environ. Microbiol.*, 2014, **16**, 255–264.

9 T. Nakagawa, R. Mitsui, A. Tani, K. Sasa, S. Tashiro, T. Iwama, T. Hayakawa and K. Kawai, A catalytic role of XoxF1 as La^{3+}-dependent methanol dehydrogenase in *Methylobacterium extorquens* strain AM1, *PLoS One*, 2012, **7**, e50480.

10 A. M. Ochsner, L. Hemmerle, T. Vonderach, R. Nüssli, M. Bortfeld-Miller, B. Hattendorf and J. A. Vorholt, Use of rare-earth elements in the phyllosphere colonizer *Methylobacterium extorquens* PA1, *Mol. Microbiol.*, 2019, **111**, 1152–1166.

11 N. C. Martinez-Gomez, H. N. Vu and E. Skovran, Lanthanide chemistry: From coordination in chemical complexes shaping our technology to coordination in enzymes shaping bacterial metabolism, *Inorg. Chem.*, 2016, **55**, 10083–10089.

12 N. M. Good, H. D. Lee, E. R. Hawker, M. Z. Su, A. A. Gilad and N. C. Martinez-Gomez, Hyperaccumulation of Gadolinium by *Methylorubrum extorquens* AM1 Reveals Impacts of Lanthanides on Cellular Processes Beyond Methylotrophy, *Front. Microbiol.*, 2022, **13**, DOI: 10.3389/fmicb.2022.820327.

13 J. T. Keltjens, A. Pol, J. Reimann and H. J. M. Op den Camp, PQQ-dependent methanol dehydrogenases: Rare-earth elements make a difference, *Appl. Microbiol. Biotechnol.*, 2014, **98**, 6163–6183.

14 L. J. Daumann, Essential and ubiquitous: The emergence of lanthanide metallobiochemistry, *Angew. Chem., Int. Ed.*, 2019, **58**, 12795–12802.

15 O. Adachi, K. Matsushita, E. Shinagawa and M. Ameyama, Purification and properties of methanol dehydrogenase and aldehyde dehydrogenase from *Methylobacillus glycogenes*, *Agric. Biol. Chem.*, 1990, **54**, 3123–3129.

16 G. E. Cozier and C. Anthony, Structure of the quinoprotein glucose dehydrogenase of *Escherichia coli* modelled on that of methanol dehydrogenase from *Methylobacterium extorquens*, *Biochem. J.*, 1995, **312**, 679–685.

17 M. Ghosh, C. Anthony, K. Harlos, M. G. Goodwin and C. Blake, The refined structure of the quinoprotein methanol dehydrogenase from *Methylobacterium extorquens* at 1.94 å, *Structure*, 1995, **3**, 177–187.

18 C. Anthony and P. Williams, The structure and mechanism of methanol dehydrogenase, *Biochim. Biophys. Acta*, 2003, **1647**, 18–23.

19 K. N. Allen and B. Imperiali, Lanthanide-tagged proteins—an illuminating partnership, *Curr. Opin. Chem. Biol.*, 2010, **14**, 247–254.

20 S. Lim and S. J. Franklin, Lanthanide-binding peptides and the enzymes that Might Have Been, *Cell. Mol. Life Sci.*, 2004, **61**, 2184–2188.

21 J. L. Gifford, M. P. Walsh and H. J. Vogel, Structures and metal-ion-binding properties of the Ca^{2+}-binding helix–loop–helix EF-hand motifs, *Biochem. J.*, 2007, **405**, 199–221.

22 J. A. Cotruvo Jr., E. R. Featherston, J. A. Mattocks, J. V. Ho and T. N. Laremore, Lanmodulin: A highly selective lanthanide-binding protein from a lanthanide-utilizing bacterium, *J. Am. Chem. Soc.*, 2018, **140**, 15056–15061.

23 E. C. Cook, E. R. Featherston, S. A. Showalter and J. A. Cotruvo Jr., Structural basis for rare earth element recognition by *Methylobacterium extorquens* lanmodulin, *Biochemistry*, 2019, **58**, 120–125.

24 E. R. Featherston, E. J. Issertell and J. A. Cotruvo, Probing lanmodulin's lanthanide recognition via sensitized luminescence yields a platform for quantification of terbium in acid mine drainage, *J. Am. Chem. Soc.*, 2021, **143**, 14287–14299.

25 H. Singer, B. Drobot, C. Zeymer, R. Steudtner and L. J. Daumann, Americium preferred: LanM, a natural lanthanide-binding protein favors an actinide over lanthanides, *Chem. Sci.*, 2021, 15581–15587.

26 G. J.-P. Deblonde, J. A. Mattocks, H. Wang, E. M. Gale, A. B. Kersting, M. Zavarin and J. A. Cotruvo, Characterization of americium and curium complexes with the protein lanmodulin: A potential macromolecular mechanism for actinide mobility in the environment, *J. Am. Chem. Soc.*, 2021, **143**, 15769–15783.

27 G. J.-P. Deblonde, J. A. Mattocks, Z. Dong, P. T. Wooddy, J. A. Cotruvo and M. Zavarin, Capturing an elusive but critical element: Natural protein enables actinium chemistry, *Sci. Adv.*, 2021, **7**, eabk0273.

28 J. T. Welch, W. R. Kearney and S. J. Franklin, Lanthanide-binding helix–turn–helix peptides: Solution structure of a designed metallonuclease, *Proc. Natl. Acad. Sci. U. S. A.*, 2003, **100**, 3725–3730.

29 M. Xu, Z. Su and J. N. Renner, Characterization of cerium (III) ion binding to surface-immobilized EF-hand loop I of calmodulin, *Pept. Sci.*, 2019, **111**, e24133.

30 J. Gariepy, B. D. Sykes and R. S. Hodges, Lanthanide-induced peptide folding: Variations in lanthanide affinity and induced peptide conformation, *Biochemistry*, 1983, **22**, 1765–1772.

31 J. Wójcik, J. Góral, K. Pawłowski and A. Bierzyński, Isolated calcium-binding loops of EF-hand proteins can dimerize to form a native-like structure, *Biochemistry*, 1997, **36**, 680–687.

32 M. Nitz, M. Sherawat, K. J. Franz, E. Peisach, K. N. Allen and B. Imperiali, Structural origin of the high affinity of a chemically evolved lanthanide-binding peptide, *Angew. Chem.*, 2004, **116**, 3768–3771.

33 L. J. Martin, B. R. Sculimbrene, M. Nitz and B. Imperiali, Rapid combinatorial screening of peptide libraries for the selection of lanthanide-binding tags (LBTs), *QSAR Comb. Sci.*, 2005, **24**, 1149–1157.

34 K. J. Franz, M. Nitz and B. Imperiali, Lanthanide-binding tags as versatile protein coexpression probes, *ChemBioChem*, 2003, **4**, 265–271.

35 M. Nitz, K. J. Franz, R. L. Maglathlin and B. Imperiali, A powerful combinatorial screen to identify high-affinity terbium(III)-binding peptides, *ChemBioChem*, 2003, **4**, 272–276.

36 B. R. Sculimbrene and B. Imperiali, Lanthanide-binding tags as luminescent probes for studying protein interactions, *J. Am. Chem. Soc.*, 2006, **128**, 7346–7352.
37 T. Hatanaka, N. Kikkawa, A. Matsugami, Y. Hosokawa, F. Hayashi and N. Ishida, The origins of binding specificity of a lanthanide ion binding peptide, *Sci. Rep.*, 2020, **10**, 19468.
38 L. Le Clainche and C. Vita, Selective binding of uranyl cation by a novel calmodulin peptide, *Environ. Chem. Lett.*, 2006, **4**, 45–49.
39 S. Sauge-Merle, F. Brulfert, R. Pardoux, P. L. Solari, D. Lemaire, S. Safi, P. Guilbaud, E. Simoni, M. L. Merroun and C. Berthomieu, Structural analysis of uranyl complexation by the EF-hand motif of calmodulin: Effect of phosphorylation, *Chem. – Eur. J.*, 2017, **23**, 15505–15517.
40 R. Pardoux, S. Sauge-Merle, D. Lemaire, P. Delangle, L. Guilloreau, J.-M. Adriano and C. Berthomieu, Modulating uranium binding affinity in engineered calmodulin EF-Hand peptides: Effect of phosphorylation, *PLoS One*, 2012, **7**, e41922.
41 G. J.-P. Deblonde, J. A. Mattocks, D. M. Park, D. W. Reed, J. A. Cotruvo and Y. Jiao, Selective and efficient biomacromolecular extraction of rare-earth elements using lanmodulin, *Inorg. Chem.*, 2020, **59**, 11855–11867.
42 Z. Dong, J. A. Mattocks, G. J.-P. Deblonde, D. Hu, Y. Jiao, J. A. Cotruvo and D. M. Park, Bridging hydrometallurgy and biochemistry: A protein-based process for recovery and separation of rare earth elements, *ACS Cent. Sci.*, 2021, **7**, 1798–1808.
43 S. J. Caldwell, I. C. Haydon, N. Piperidou, P.-S. Huang, M. J. Bick, H. S. Sjöström, D. Hilvert, D. Baker and C. Zeymer, Tight and specific lanthanide binding in a *de novo* TIM barrel with a large internal cavity designed by symmetric domain fusion, *Proc. Natl. Acad. Sci. U. S. A.*, 2020, **117**, 30362–30369.
44 L. N. Slope, O. J. Daubney, H. Campbell, S. A. White and A. Peacock, Location dependent lanthanide selectivity engineered into structurally characterized designed coiled coils, *Angew. Chem., Int. Ed.*, 2021, **60**, 14473–24477.
45 H. Lumpe, A. Menke, C. Haisch, P. Mayer, A. Kabelitz, K. V. Yusenko, A. G. Buzanich, T. Block, R. Pöttgen, F. Emmerling and L. J. Daumann, The earlier the better: Structural analysis and separation of lanthanides with pyrroloquinoline quinone, *Chem. – Eur. J.*, 2020, **26**, 10133–10139.
46 D. B. Halling, B. J. Liebeskind, A. W. Hall and R. W. Aldrich, Conserved properties of individual Ca^{2+}-binding sites in calmodulin, *Proc. Natl. Acad. Sci. U. S. A.*, 2016, **113**, E1216–E1225.
47 S. K. Drake, K. L. Lee and J. J. Falke, Tuning the equilibrium ion affinity and selectivity of the EF-Hand calcium binding motif: Substitutions at the gateway position, *Biochemistry*, 1996, **35**, 6697–6705.
48 S. K. Drake and J. J. Falke, Kinetic tuning of the EF-Hand calcium binding motif: The gateway residue independently adjusts (i) barrier height and (ii) equilibrium, *Biochemistry*, 1996, **35**, 1753–1760.
49 R. C. Hapak, P. J. Lammers, W. A. Palmisano, E. R. Birnbaum and M. T. Henzl, Site-specific substitution of glutamate for aspartate at position 59 of rat oncomodulin, *J. Biol. Chem.*, 1989, **264**, 18751–18760.
50 S. Liu, E. R. Featherston, J. A. Cotruvo and C. R. Baiz, Lanthanide-dependent coordination interactions in lanmodulin: A 2D IR and molecular dynamics simulations study, *Phys. Chem. Chem. Phys.*, 2021, 21690–21700.
51 D. Muralidhar, M. Kunjachen Jobby, A. Jeromin, J. Roder, F. Thomas and Y. Sharma, Calcium and chlorpromazine binding to the EF-hand peptides of neuronal calcium sensor-1, *Peptides*, 2004, **25**, 909–917.
52 R. Dölling, M. Beyermann, J. Haenel, F. Kernchen, E. Krause, P. Franke, M. Brudel and M. Bienert, Piperidine-mediated side product formation for Asp(OBut)-containing peptides, *J. Chem. Soc., Chem. Commun.*, 1994, 853–854.
53 R. Behrendt, P. White and J. Offer, Advances in Fmoc solid-phase peptide synthesis, *J. Pept. Sci.*, 2016, **22**, 4–27.
54 J. L. Lauer, C. G. Fields and G. B. Fields, Sequence dependence of aspartimide formation during 9-fluorenylmethoxycarbonyl solid-phase peptide synthesis, *Lett. Pept. Sci.*, 1995, **1**, 197–205.
55 D. Samson, D. Rentsch, M. Minuth, T. Meier and G. Loidl, The aspartimide problem persists: Fluorenylmethyloxycarbonyl-solid-phase peptide synthesis (Fmoc-SPPS) chain termination due to formation of N-terminal piperazine-2,5-diones, *J. Pept. Sci.*, 2019, **25**, e3193.
56 T. Michels, R. Dölling, U. Haberkorn and W. Mier, Acid-mediated prevention of aspartimide formation in solid phase peptide synthesis, *Org. Lett.*, 2012, **14**, 5218–5221.
57 B. Drobot, M. Schmidt, Y. Mochizuki, T. Abe, K. Okuwaki, F. Brulfert, S. Falke, S. A. Samsonov, Y. Komeiji, C. Betzel, T. Stumpf, J. Raff and S. Tsushima, Cm^{3+}/Eu^{3+} induced structural, mechanistic and functional implications for calmodulin, *Phys. Chem. Chem. Phys.*, 2019, **21**, 21213–21222.
58 R. E. Reid, D. M. Clare and R. S. Hodges, Synthetic analog of a high affinity calcium binding site in rabbit skeletal troponin C., *J. Biol. Chem.*, 1980, **255**, 3642–3646.
59 S. Yokokawa, S. Tsubuki, H. Ito and H. Kasai, The synthesis and properties of EF-hand type calcium-binding peptides, *Chem. Lett.*, 1989, **18**, 1627–1630.
60 P. Kanellis, J. Yang, H. C. Cheung and R. E. Lenkinski, Synthetic peptide analogs of skeletal troponin C: Fluorescence studies of analogs of the low-affinity calcium-binding site II, *Arch. Biochem. Biophys.*, 1983, **220**, 530–540.
61 N. A. Malik, G. M. Anantharamaiah, A. Gawish and H. C. Cheung, Structural and biological studies on synthetic peptide analogues of a low-affinity calcium-binding site of skeletal troponin C, *Biochim. Biophys. Acta, Protein Struct. Mol. Enzymol.*, 1987, **911**, 221–230.
62 W. C. Johnson, Secondary structure of proteins through circular dichroism spectroscopy, *Annu. Rev. Biophys. Biophys. Chem.*, 1988, 145–166.
63 R. E. Reid, J. Gariépy, A. K. Saund and R. S. Hodges, Calcium-induced protein folding. Structure–affinity

relationships in synthetic analogs of the helix–loop–helix calcium binding unit., *J. Biol. Chem.*, 1981, **256**, 2742–2751.
64 G. Borin, P. Ruzza, M. Rossi, A. Calderan, F. Marchiori and E. Peggion, Conformation and ion binding properties of peptides related to calcium binding domain III of bovine brain calmodulin, *Biopolymers*, 1989, **28**, 353–369.
65 P. Kantakevičius, C. Mathiah, L. O. Johannissen and S. Hay, Chelator-based parameterization of the 12–6–4 Lennard–Jones molecular mechanics potential for more realistic metal ion–protein interactions, *J. Chem. Theory Comput.*, 2022, **18**, 2367–2374.
66 T. Kimura and G. R. Choppin, Luminescence study on determination of the hydration number of Cm(III), *J. Alloys Compd.*, 1994, **213–214**, 313–317.
67 W. DeW. Horrocks and D. R. Sudnick, Lanthanide ion probes of structure in biology. Laser-induced luminescence decay constants provide a direct measure of the number of metal-coordinated water molecules, *J. Am. Chem. Soc.*, 1979, **101**, 334–340.
68 S. Özçubukçu, K. Mandal, S. Wegner, M. P. Jensen and C. He, Selective recognition of americium by peptide-based reagents, *Inorg. Chem.*, 2011, **50**, 7937–7939.